Parametric modelling of the dynamic behaviour of a steel–concrete composite floor

José G.S. da Silva [a,*], Sebastião A.L. de Andrade [b], Elvis D.C. Lopes [a]

[a] State University of Rio de Janeiro, Structural Engineering Department, Brazil
[b] Pontifical Catholic University of Rio de Janeiro, Civil Engineering Department, Brazil

ABSTRACT

Nowadays the new architecture tendencies and construction market demands are leading the structural engineers to search for increasingly daring solutions. These new structural systems are intrinsically associated to the recent evolution of building construction methods, i.e. fast erection and assembly, with minimum weight, being capable of supporting large spans with few columns enabling greater constructed space flexibility. A direct consequence of this new design trend is the increasing incidence of building vibration problems due to human activities. This was the main motivation for the development of a design methodology centred on the modelling of the dynamic behaviour of steel–concrete composite floors submitted to loads due to human rhythmic activities for the evaluation of human comfort. Thus, three dynamic loading models were utilised to simulate human rhythmic activities such as jumping and aerobics. The dynamic loads were obtained through experimental tests and were based on international design codes and recommendations. The investigated structural model was based on a real steel–concrete composite floor spanning 40 m by 40 m, with a total area of 1600 m^2. The structural system consisted of a typical composite floor of a commercial building. The peak accelerations values found in the present investigation indicated that human rhythmic activities could induce the composite floors to reach unacceptable vibration levels leading to a violation of the current human comfort criteria.

© 2014 Elsevier Ltd. All rights reserved.

1. Introduction

Currently, steel and steel–concrete composite building structures are increasingly becoming the modern landmarks of urban areas. Designers seem to continuously move the safety border to increase slenderness and lightness of their structural systems [1–15]. However, more and more steel and composite floors are constructed as light-weight structures with low frequencies and low damping [1–15]. These practices have generated very slender composite floors sensitive to dynamic excitation and consequently changed the serviceability and ultimate limit states associated with their design [16–22].

A direct consequence of this new design trend is a considerable increase in problems related to unwanted composite floor vibrations. For this reason, the structural flooring systems become vulnerable to excessive vibrations produced by impacts such as human rhythmic activities [1–15]. Due to the above mentioned aspects a consistent structural analysis of the composite floors dynamic behaviour is advisable. These design aspects have led

structural designers to verify the resistance and stability of the structural systems that do not exceed their ultimate limit states [16–22].

The vibration problems related to these composite floors serviceability limit states should be analysed with caution, searching for viable alternatives to minimise the human activities vibration effects. This was the main motivation for the development of a design methodology centred on the modelling of the dynamic behaviour of steel–concrete composite floors submitted to loads due to human rhythmic activities for the evaluation of human comfort.

The dynamic loads were obtained through experimental tests with individuals conducting rhythmic and non-rhythmic activities, such as stimulated and non-stimulated jumping and aerobics [25]. Based on the experimental results, human load functions due to rhythmic and non-rhythmic activities are proposed [25].

The investigated structural model was based on a real steel–concrete composite floor spanning 40 m by 40 m. In this investigation, the commercial software ANSYS [26] was used to perform finite element analyses. It must be emphasised that the structural behaviour of the connections (beam-to-column and beam-to-beam connections) and also the steel–concrete interaction degree (from

* Corresponding author. Tel./fax: +55 21 23340080.
  E-mail addresses: jgss@uerj.br, jgss@eng.uerj.br (J.G.S. da Silva).

full to partial interaction cases) were incorporated in the finite element modelling of the investigated composite floor dynamic response.

Initially, all the composite floor natural frequencies and vibration modes were obtained. Based on an extensive parametric study, the floor dynamic response in terms of peak accelerations was obtained and compared to the limiting values proposed by several authors and design codes [23,24,27–30]. The current investigation indicated that human rhythmic activities could induce the steel–concrete composite floors to reach unacceptable vibration levels and, in these situations, could lead to a violation of the current human comfort criteria for these specific structures.

2. Dynamic loading induced by human rhythmic activities

The description of the dynamic loads generated by human rhythmic activities is not a simple task. The individual characteristics in which each individual performs the same activity and the existence of external excitation are key factors in defining the dynamic action characteristics. Numerous investigations were made aiming to establish parameters to describe such dynamic actions [1–15,23,24,27].

Human loads comprise a large portion of the acting live loads in offices, commercial and residential building floors. In general, human live loads are classified into two broad categories: in situ and moving. Periodic jumping due to music, sudden standing of a crowd, and random in-place movements are examples of in situ activities. Walking, marching, and running are examples of moving activities. As the main purpose of the steel–concrete composite floors is supporting moving activities of humans, they must be safe and comfortable for users [1–15].

However, human activities produce dynamic forces, and their associated vibration levels should not disturb or alarm the building's occupants. Therefore, this investigation describes three different loading models developed to incorporate the dynamic effects induced by human rhythmic activities on the steel–concrete composite floor's dynamic response.

2.1. Loading model I (LM-I)

Several investigations have described the loading generated by human activities as a Fourier series, which considers a static part due to the individual's weight and another part due to the dynamic load [1–15]. The dynamic analysis is performed by equating one of the activity harmonics to the floor fundamental frequency, leading to resonance.

This study considered the dynamic loads obtained by Faisca [25], based on the results achieved through a long series of experimental tests with individuals performing rhythmic and non-rhythmic activities. The dynamic loads generated by human rhythmic activities such as stimulated and non-stimulated jumping, aerobics, football crowds, spectators in concerts and dancing were investigated by Faisca [25].

In this paper, the Hanning function was used to represent the human dynamic actions. The Hanning function was used because it was verified that this mathematical representation is very similar to the signal force obtained through experimental tests developed by Faisca [25].

The mathematical representation of the human dynamic loading using the Hanning function is given by Eq. (1).

In this dynamic loading model, three harmonics were considered to represent the load associated with human rhythmic activities. It is important to emphasise that the impact coefficient, K_p, and the phase coefficient variation, CD, for human activities used in this investigation were obtained based on a long series of

experimental tests and probabilistic analyses. Relevant variations which lead to the reduction of the dynamic loading on the floor, such as phase lags between the individuals and change of rhythm during the activity are already embedded in these coefficients, see Eq. (1).

$$F(t) = CD\left\{K_p P\left[0.5 - 0.5\cos\left(\frac{2\pi}{T_c}t\right)\right]\right\} \quad \text{when } t \leq T_c$$
$$F(t) = 0 \qquad\qquad\qquad\qquad\qquad \text{when } T_c \leq t \leq T \tag{1}$$

Here, $F(t)$: dynamic load (N); CD: phase coefficient; K_p: impact coefficient; P: person's weight; T_c: activity contact period (s); T: activity period (s); t: time (s).

This way, Fig. 1 illustrates the phase coefficient variation, CD, for human activities studied by Faisca [25], considering a certain number of individuals and later extrapolated for a large number of people, based on probabilistic analyses. Fig. 2 presents some examples of the dynamic actions related to human rhythmic activities (aerobics, free jumps and rock concert), illustrating the three harmonics considered in this loading model, when a frequency domain analysis was performed.

2.2. Loading model II (LM-II)

This dynamic loading model can be represented by the load static parcel, related to the individual's weight, and a combination of harmonic forces with frequencies that are multiples or harmonics of the basic frequency of the force repetition, e.g., step frequency, f_s, for human rhythmic activities [27]. This loading model considers a spatial and temporal variation of the dynamic action over the structure, and the time-dependent repeated force can be represented by the Fourier series in Eq. (2).

$$F(t) = P\left[1 + \sum \alpha_i \cos(2\pi i f_s t + \phi_i)\right] \tag{2}$$

Here, $F(t)$: dynamic load (N); P: person's weight; α_i: dynamic coefficient for the harmonic force; i: harmonic multiple ($i = 1, 2, 3\ldots, n$); f_s: walking step frequency (Hz); ϕ_i: harmonic phase angle; t: time (s).

In this load model, three harmonics were considered to represent the dynamic load associated with human rhythmic activities. In this mathematical model, the phase angles were assumed to be equal to zero [27]. Fig. 3 illustrates a representation of the dynamic loading induced by human rhythmic activities (aerobics).

2.3. Loading model III (LM-III)

In this case, a general expression is used to represent the excitation produced by an individual practising rhythmic activity over time. These loads are produced with both feet, as a function of a static part associated with the individual's weight and as three harmonics representing the dynamic action related to human
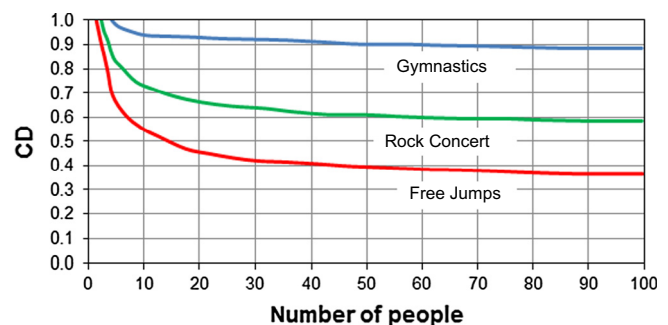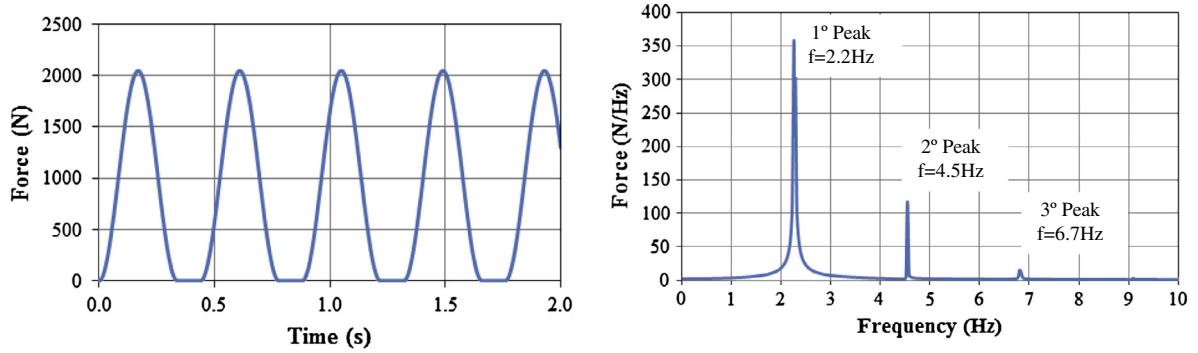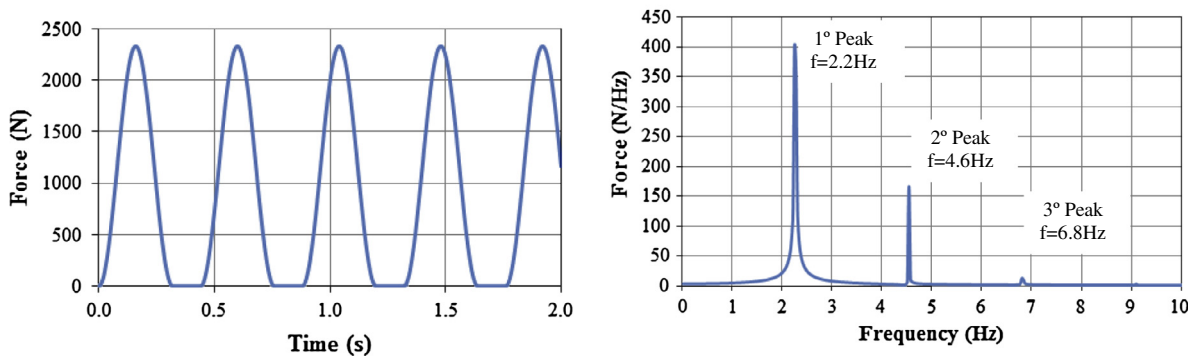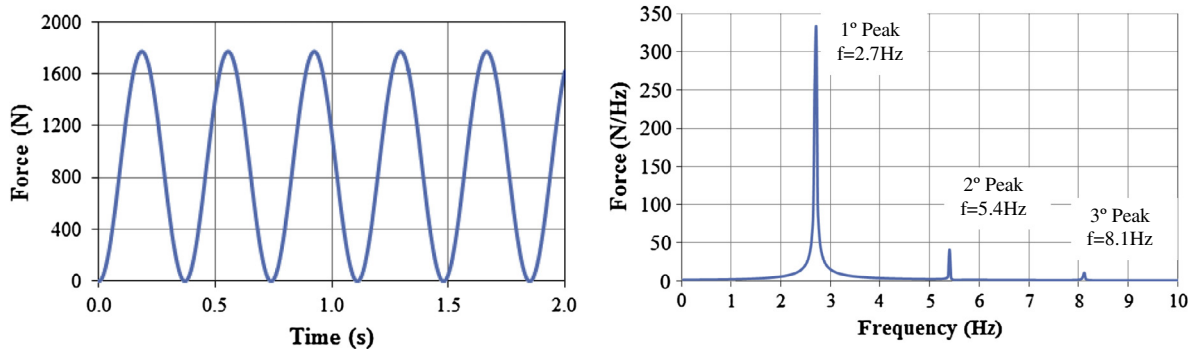

Fig. 1. Variation of the phase coefficient CD for human rhythmic activities [20].

(a) Aerobics: T = 0.44s, T_c = 0.34s, K_p = 2.78, CD = 0.92.

(b) Free Jumps: T = 0.44s, T_c = 0.32s, K_p = 3.17, CD = 0.92.

(c) Rock Concert: T = 0.37s, T_c = 0.33s, K_p = 2.41, CD = 0.92.

Fig. 2. Dynamic loading induced by human rhythmic activities (LM-I).
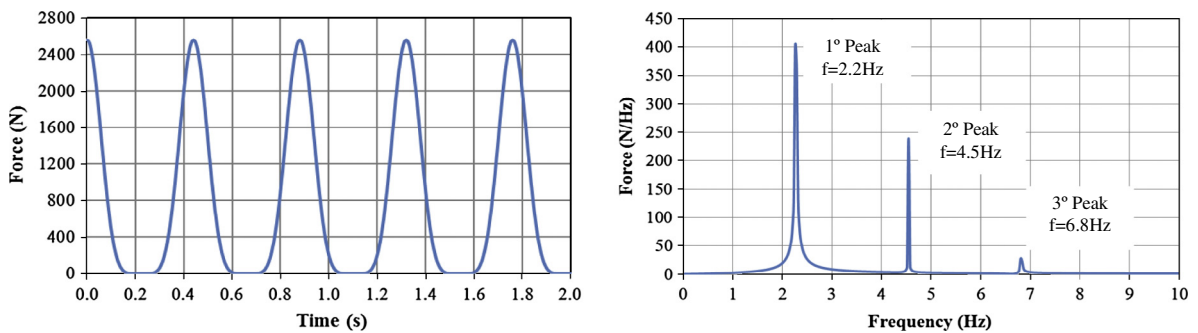
Fig. 3. Dynamic loading induced by human rhythmic activities (LM-II). Aerobics: f_p = 2.27 Hz, α_1 = 1.5, α_2 = 0.6, α_3 = 0.1, $\phi_1 = \phi_2 = \phi_3 = 0$.

rhythmic activities [30], as illustrated in Eq. (3). This loading model considers spatial and temporal variations of the dynamic action over the floor.

$$F(t) = P + \Delta_1 P \sin(2\pi f_s t - \phi_1) + \Delta_2 P \sin(4\pi f_s t - \phi_2)$$
$$+ \Delta_3 P \sin(6\pi f_s t - \phi_3)$$

(3)
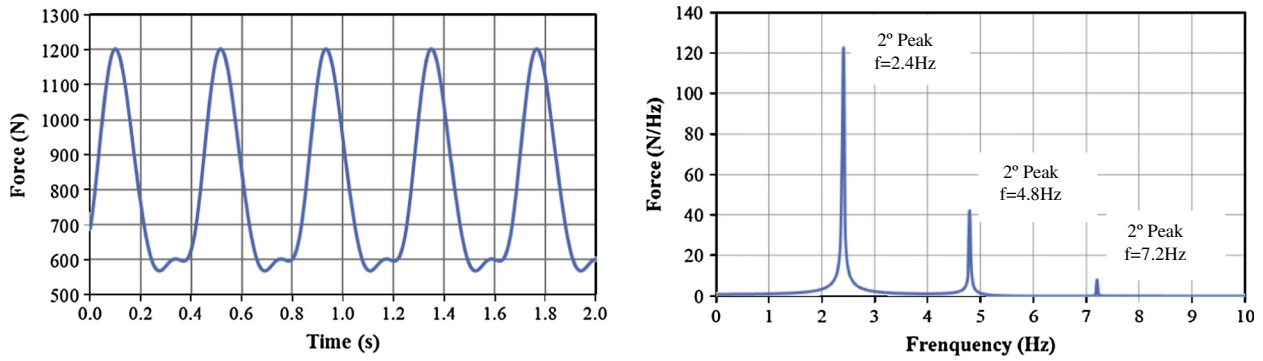
(a) $f_p = 2.40$Hz, $\phi_1 = 0$, $\phi_2 = 1.57$, $\phi_3 = 1.57$, $\alpha_1 = 0.38$, $\alpha_2 = 0.12$, $\alpha_3 = 0.02$.

Fig. 4. Dynamic loading induced by human rhythmic activities (LM-III). Aerobics: $f_p = 2.40$ Hz; $\Delta_1 = 0.38$; $\Delta_2 = 0.12$; $\Delta_3 = 0.02$; $\phi_1 = 0$; $\phi_2 = \pi/2$; $\phi_3 = \pi/2$.

■: Nodes A to H for the obtained dynamic response   ●: 32 people practising aerobics
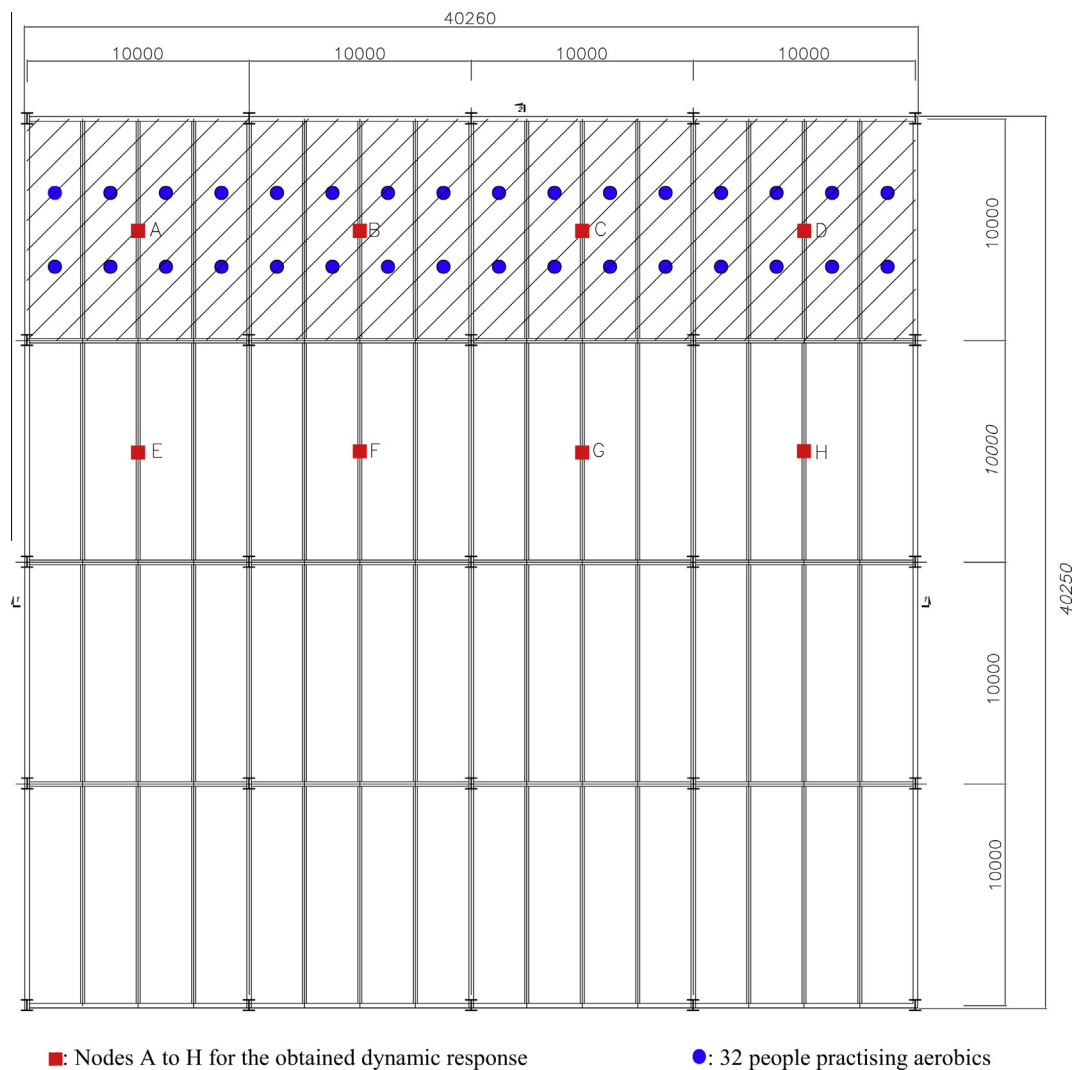
Fig. 5. Investigated structural model: steel–concrete composite floor plan. Dimensions in (mm).

Here, $F(t)$: loading function varying in time; P: person's weight; Δ_i: Fourier coefficient for the harmonic; i: harmonic multiple ($i = 1, 2, 3,...,n$); $\Delta_i P$: loading amplitude corresponding to the ith harmonic; f_s: human step frequency; ϕ_i: phase angle for harmonic i; t: time.

It must be emphasised that a large scatter exists in experimentally determined phase angles [7,12,23,24]. The phase angles ϕ_2 and ϕ_3 depend on various other factors and should represent the most unfavourable combination of the different harmonics [23,24]. In the present study, phase angles ϕ_2 and ϕ_3 were assumed to be equal to $\pi/2$, and phase angle ϕ_1 was assumed to be equal to zero [30]. Fig. 4 presents a representation of the dynamic loading induced by human rhythmic activities (aerobics).
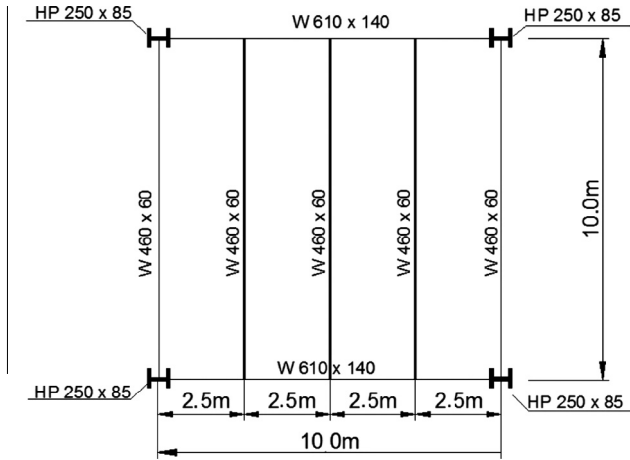
(a) Generic interior bay floor framing details.
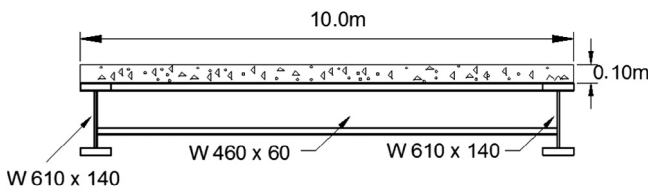
(b) Generic interior bay floor framing cross section.

Fig. 6. Investigated steel–concrete composite floor.
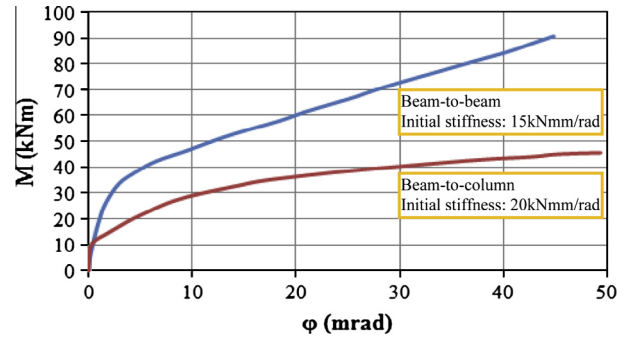
Fig. 8. Moment versus rotation curve: beam-to-beam semi-rigid connections [26] and beam-to-column semi-rigid connections [27].
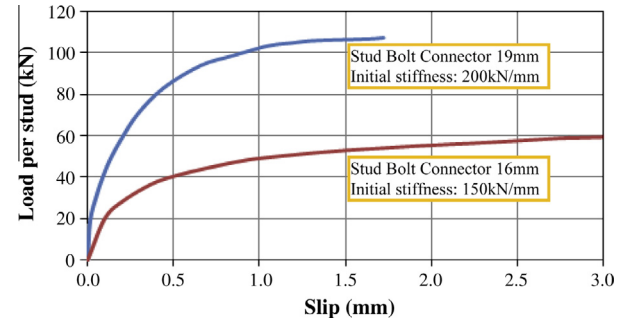
Fig. 9. Force versus slip curve of the investigated shear connectors: Stud bolt connectors of 16 mm and 19 mm [28–30].

Table 1
Geometric characteristics of the building composite floor (mm).

Profile type	Height (d)	Flange width (b_f)	Top flange thickness (t_f)	Bottom flange thickness (t_f)	Web thickness (t_w)
Main beams: (W610 × 140)	617	230	22.2	22.2	13.1
Secondary beams: (W460 × 60)	455	153	13.3	13.3	8.0
Columns: (HP250 × 85)	254	260	14.4	14.4	14.4
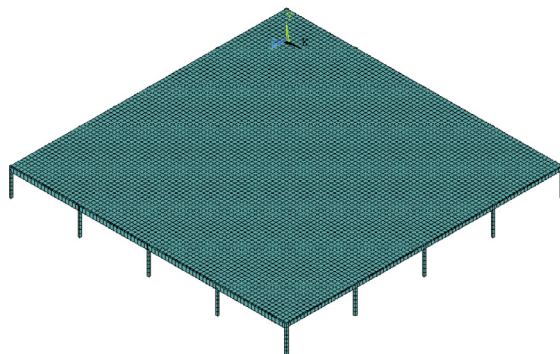
(a) Finite element model.
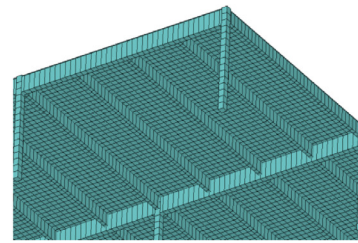
(b) Bottom view.
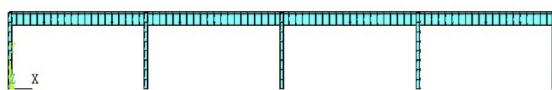
(c) Plan XY view.

Elements	= 32036
Beam44	= 3920
Shell63	= 25600
Combin39	= 2516
Nodes	= 29874
DOF	= 166589

Fig. 7. Steel–concrete composite floor finite element model.

Table 2
Composite floor natural frequencies. Beam-to-column rigid connections. Stud 16 mm: S_j = 150 kN/mm.

Frequencies (Hz)	Total interaction			Partial interaction (50%)		
	Rigid	Semi-rigid	Flexible	Rigid	Semi-rigid	Flexible
f_{01}	0.71	0.71	0.71	0.71	0.71	0.71
f_{02}	1.21	1.19	1.19	1.21	1.19	1.19
f_{03}	1.21	1.21	1.21	1.21	1.20	1.21
f_{04}	6.65	6.20	6.07	6.41	5.99	5.86
f_{05}	6.76	6.48	6.37	6.54	6.27	6.15
f_{06}	7.12	6.60	6.45	6.87	6.37	6.21
f_{07}	7.14	6.78	6.66	6.87	6.56	6.42
f_{08}	7.18	7.03	6.93	6.96	6.81	6.69
f_{09}	7.35	7.17	7.06	7.10	6.92	6.80
f_{10}	7.39	7.25	7.12	7.13	6.98	6.85

Table 3
Composite floor natural frequencies. Beam-to-column rigid connections. Stud 19 mm: S_j = 200 kN/mm.

Frequencies (Hz)	Total interaction			Partial interaction (50%)		
	Rigid	Semi-rigid	Flexible	Rigid	Semi-rigid	Flexible
f_{01}	0.71	0.71	0.71	0.71	0.71	0.71
f_{02}	1.21	1.19	1.19	1.21	1.19	1.19
f_{03}	1.21	1.21	1.21	5.64	1.20	1.21
f_{04}	6.63	6.18	6.06	6.39	5.98	5.84
f_{05}	6.75	6.46	6.36	6.52	6.26	6.13
f_{06}	7.10	6.58	6.43	6.84	6.35	6.19
f_{07}	7.11	6.77	6.65	6.85	6.54	6.40
f_{08}	7.17	7.02	6.91	6.94	6.79	6.67
f_{09}	7.35	7.16	7.05	7.08	6.91	6.78
f_{10}	7.38	7.24	7.11	7.11	6.97	6.83

Table 4
Composite floor natural frequencies. Beam-to-column semi-rigid connections: S_j = 20 kN mm/rad. Stud 16 mm: S_j = 150 kN/mm.

Frequencies (Hz)	Total interaction			Partial interaction (50%)		
	Rigid	Semi-rigid	Flexible	Rigid	Semi-rigid	Flexible
f_{01}	0.72	0.72	0.72	0.72	0.72	0.72
f_{02}	1.11	1.09	1.08	1.11	1.09	1.08
f_{03}	1.12	1.10	1.09	1.12	1.10	1.09
f_{04}	6.40	5.96	5.83	6.13	5.76	5.62
f_{05}	6.52	6.22	6.12	6.28	6.04	5.92
f_{06}	6.90	6.34	6.19	6.60	6.14	5.97
f_{07}	6.90	6.51	6.40	6.63	6.31	6.18
f_{08}	6.97	6.77	6.69	6.74	6.57	6.47
f_{09}	7.17	6.90	6.82	6.91	6.69	6.58
f_{10}	7.26	7.04	6.85	7.01	6.81	6.60

Table 5
Composite floor natural frequencies. Beam-to-column semi-rigid connections: S_j = 20 kN mm/rad. Stud 19 mm: S_j = 200 kN/mm.

Frequencies (Hz)	Total interaction			Partial interaction (50%)		
	Rigid	Semi-rigid	Flexible	Rigid	Semi-rigid	Flexible
f_{01}	0.72	0.72	0.72	0.72	0.72	0.72
f_{02}	1.11	1.09	1.08	1.11	1.09	1.08
f_{03}	1.12	1.10	1.09	1.12	1.10	1.09
f_{04}	6.37	5.94	5.82	6.10	5.76	5.61
f_{05}	6.50	6.21	6.11	6.25	6.03	5.91
f_{06}	6.87	6.33	6.17	6.57	6.13	5.95
f_{07}	6.88	6.50	6.39	6.60	6.30	6.16
f_{08}	6.95	6.76	6.67	6.72	6.56	6.45
f_{09}	7.15	6.89	6.81	6.88	6.67	6.56
f_{10}	7.25	7.02	6.83	6.99	6.79	6.58

(a) Secondary beams. Stud 16mm: $S_j = 150$kN/mm.

(b) Secondary beams. Stud 19mm: $S_j = 200$kN/mm.

(c) Main beams. Stud 16mm: $S_j = 150$kN/mm.

(d) Main beams. Stud 19mm: $S_j = 200$kN/mm.

(e) Combinations between the main and secondary beams [1]. Stud 16mm.

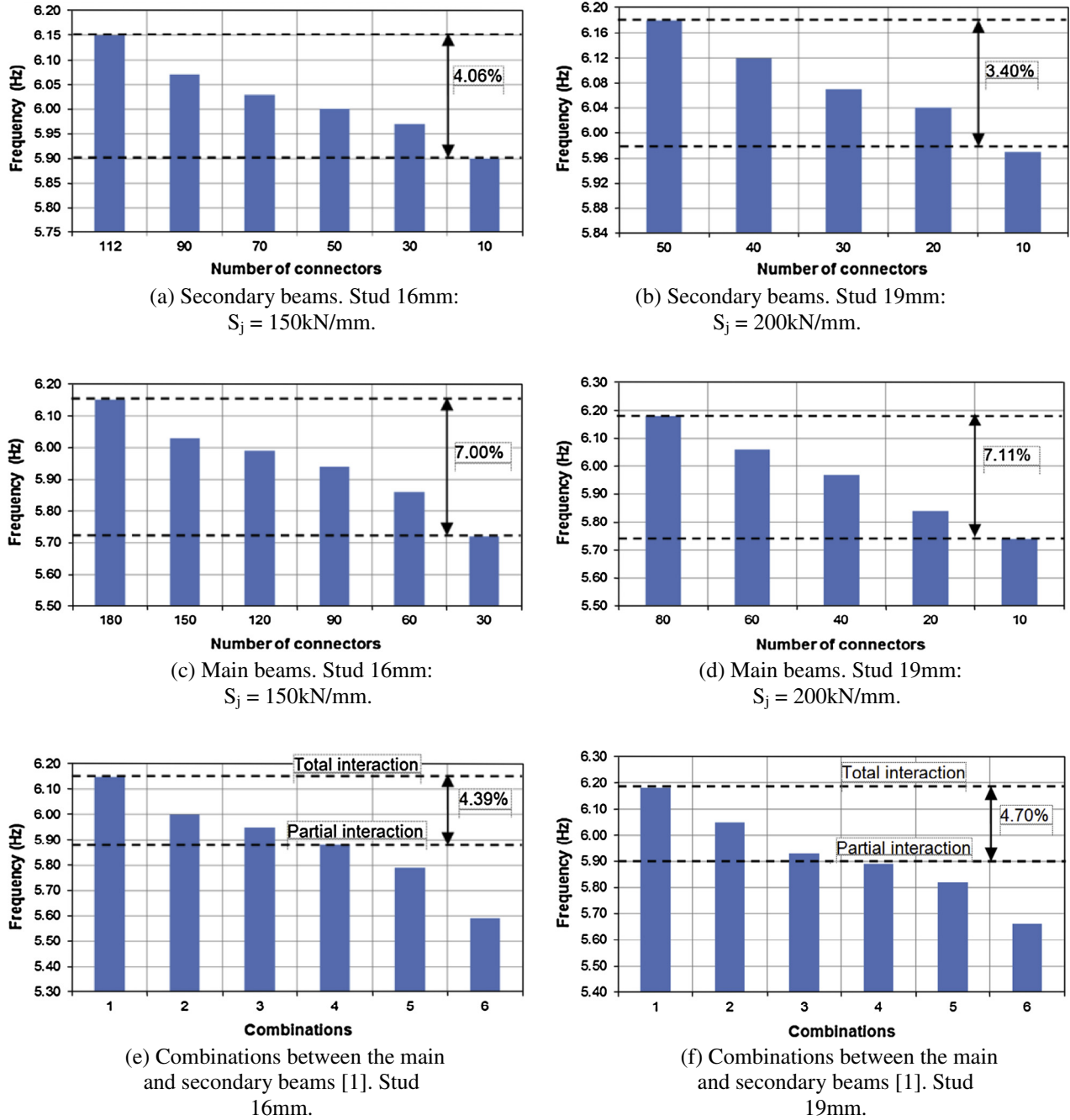(f) Combinations between the main and secondary beams [1]. Stud 19mm.

Fig. 10. Steel–concrete composite floor fundamental frequency (f_{01}) variation.

3. Investigated structural model

The investigated structural model was based on a real steel–concrete composite floor spanning 40 m by 40 m, with a total area of 1600 m^2 [1,16]. The structural system consisted of a typical composite floor of a commercial building. The floor studied in this work is supported by steel columns and is currently submitted to human rhythmic loads. The model is constituted of composite girders and a 100 mm (0.10 m) thick concrete slab [1,16], see Figs. 5 and 6.

The steel sections were welded wide flanges (WWF) made with a 345 MPa yield stress steel grade. A 2.05×10^5 MPa Young's modulus was adopted for the steel beams. The concrete slab has a 30 MPa specified compression strength and a 2.6×10^4 MPa

Young's modulus. Table 1 depicts the geometric characteristics of the steel beams and columns.

The human-induced dynamic load was applied on the aerobics area. The composite floor dynamic response, in terms of peak accelerations values, was obtained on nodes A to H to verify the influence of the dynamic load on the adjacent slab floors, as presented in Fig. 5.

In this investigation, the dynamic loadings were applied to the structural model corresponding to the effect of thirty-two individuals practising aerobics. The live load considered in this analysis corresponds to one person for each 4.0 m^2 (0.25 person/m^2) [23,24]. The load distribution was considered symmetrically centred on the slab panels, see Fig. 5. It is also assumed that an individual person's weight is equal to 800 N (0.8 kN) [23,24].
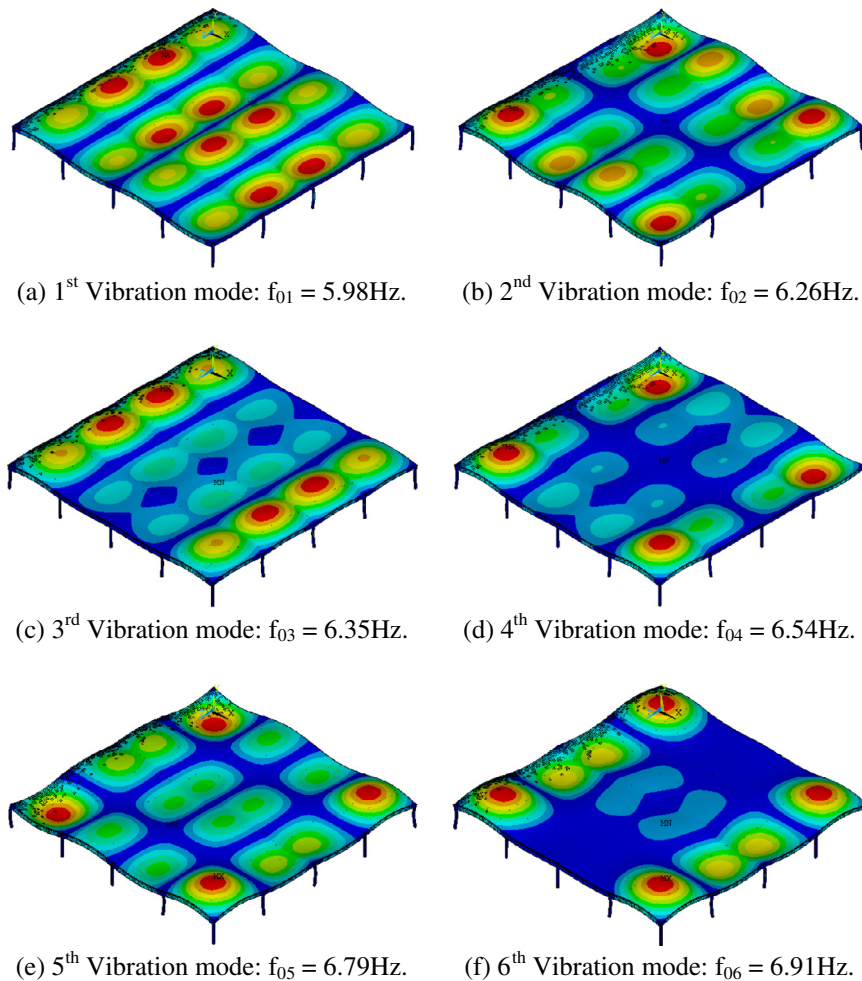
(a) 1st Vibration mode: $f_{01} = 5.98$Hz.

(b) 2nd Vibration mode: $f_{02} = 6.26$Hz.

(c) 3rd Vibration mode: $f_{03} = 6.35$Hz.

(d) 4th Vibration mode: $f_{04} = 6.54$Hz.

(e) 5th Vibration mode: $f_{05} = 6.79$Hz.

(f) 6th Vibration mode: $f_{06} = 6.91$Hz.

Fig. 11. Vibration modes of the structural model. Steel–concrete: partial interaction. Beam-to-column connections: rigid. Beam-to-beam connections: semi-rigid. Stud: 19 mm.

4. Finite element modelling

The proposed computational model, developed for the composite floor dynamic analysis, adopted the usual mesh refinement techniques present in finite element method simulations implemented in the ANSYS program [26]. This numerical model enabled a complete dynamic evaluation of the investigated steel–concrete composite floor, especially in terms of human comfort and its associated vibration serviceability limit states. The present investigation considered that both materials (steel and concrete) have an elastic behaviour. The finite element model of the investigated steel–concrete composite floor is illustrated in Fig. 7.

In this computational model, all "I" steel sections related to beams and columns were represented by three-dimensional beam elements (BEAM44 [26]) with tension, compression, torsion and bending capabilities. The reinforced concrete slab was represented by shell finite elements (SHELL63 [26]) with both bending and membrane capabilities. Both in-plane and normal loads are permitted.

The structural behaviour of the beam-to-column and beam-to-beam connections (rigid, semi-rigid and flexible) present in the investigated steel–concrete composite floor was simulated by non-linear spring elements (COMBIN7 and COMBIN39 [26]), which incorporate the geometric non-linearity and the hysteretic behaviour effects. The moment-versus-rotation curve related to the adopted semi-rigid connections was based on experimental data [31,32], as shown in Fig. 8.

When the complete interaction between the concrete slab and steel beams was considered in the analysis, the composite floor finite element model coupled all the nodes between the beams and slab to prevent the occurrence of any slip. However, to enable the slip between the concrete slab and the "I" steel profiles to represent the partial interaction (steel–concrete) cases, the modelling strategy used non-linear spring elements (COMBIN39 [26]) that simulated the shear connector actions. The adopted shear connector force-versus-displacement curves were also based on experimental tests [33–35], as illustrated in Fig. 9.

The final computational model used 27,569 nodes and 29,616 finite elements, 3920 three-dimensional beam elements, 25,600 shell elements and 96 spring elements, which resulted in a numeric model with 164,809 degrees of freedom.

5. Composite floor structural damping

The structural damping in a steel–concrete composite floor system is a very important parameter in dynamic problems, especially in mitigating its excessive vibration. Although damping in a composite floor system can be measured using the heel impact test a precise value for the structural damping in steel–concrete composite floor systems is mostly unknown due to various limitations. However, there are a lot of references reporting several damping levels in the technical literature and in general, damping for composite floors is defined to be between 1.0% and 2.0% [1,6,23,24,27,36].
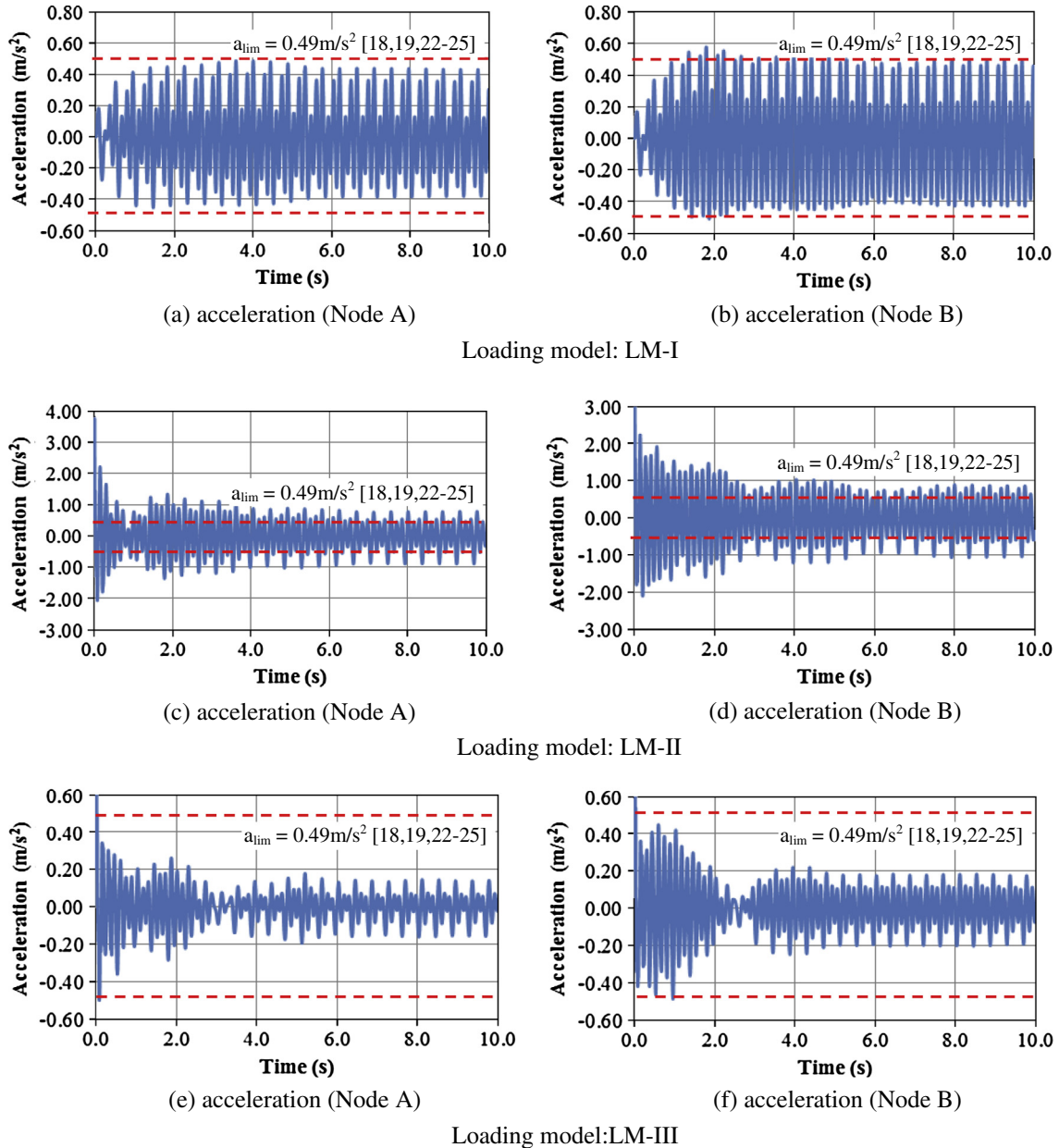
(a) acceleration (Node A)

(b) acceleration (Node B)

Loading model: LM-I

(c) acceleration (Node A)

(d) acceleration (Node B)

Loading model: LM-II

(e) acceleration (Node A)

(f) acceleration (Node B)

Loading model:LM-III

Fig. 12. Structural model displacements and accelerations. Steel–concrete: partial interaction. Beam-to-column connections: rigid. Beam-to-beam connections: semi-rigid. Stud: 19 mm.

In this investigation, the structural damping was considered according to the Rayleigh proportional damping formulation [37]. The composite floor damping matrix is defined by the parameters α and β, determined in the function of the damping modal coefficient. According to this formulation, the structural system damping matrix is proportional to the mass and stiffness matrix, as shown in Eq. (4):

$$[C] = \alpha[M] + \beta[K] \tag{4}$$

The expression above can be rewritten in terms of the modal damping coefficient and the natural frequency, leading to Eq. (5):

$$\xi_i = \frac{\alpha}{2\omega_i} + \frac{\beta\omega_i}{2} \tag{5}$$

where ξ_i is the modal damping ratio for mode shape "i" and ω_i is the natural frequency associated with mode shape "i". Isolating the Eq. (5) parameters α and β for two natural frequencies ω_{01}

and ω_{02}, adopted according to the relevance of the corresponding vibration mode for the structural system dynamic response, generates:

$$\beta = \frac{2(\xi_2\omega_{02} - \xi_1\omega_{01})}{\omega_{02}\omega_{02} - \omega_{01}\omega_{01}} \tag{6}$$

$$\alpha = 2\xi_1\omega_{01} - \beta\omega_{01}\omega_{01} \tag{7}$$

With two natural frequency values, it is possible to evaluate the parameters α and β described before using Eqs. (6) and (7). The reference frequencies ω_{01} and ω_{02} are generally taken as the extreme frequencies of the structure spectrum. In this paper, the adopted frequency ω_{01} will be the structure's fundamental frequency, and the considered frequency ω_{02} will be the system's 2nd natural frequency. The modal damping ratio adopted in this investigation for the composite floor first and second vibration modes is equal to 0.01 ($\xi = \xi_1 = \xi_2 = 1\%$) [1,6,23,24,27,36].
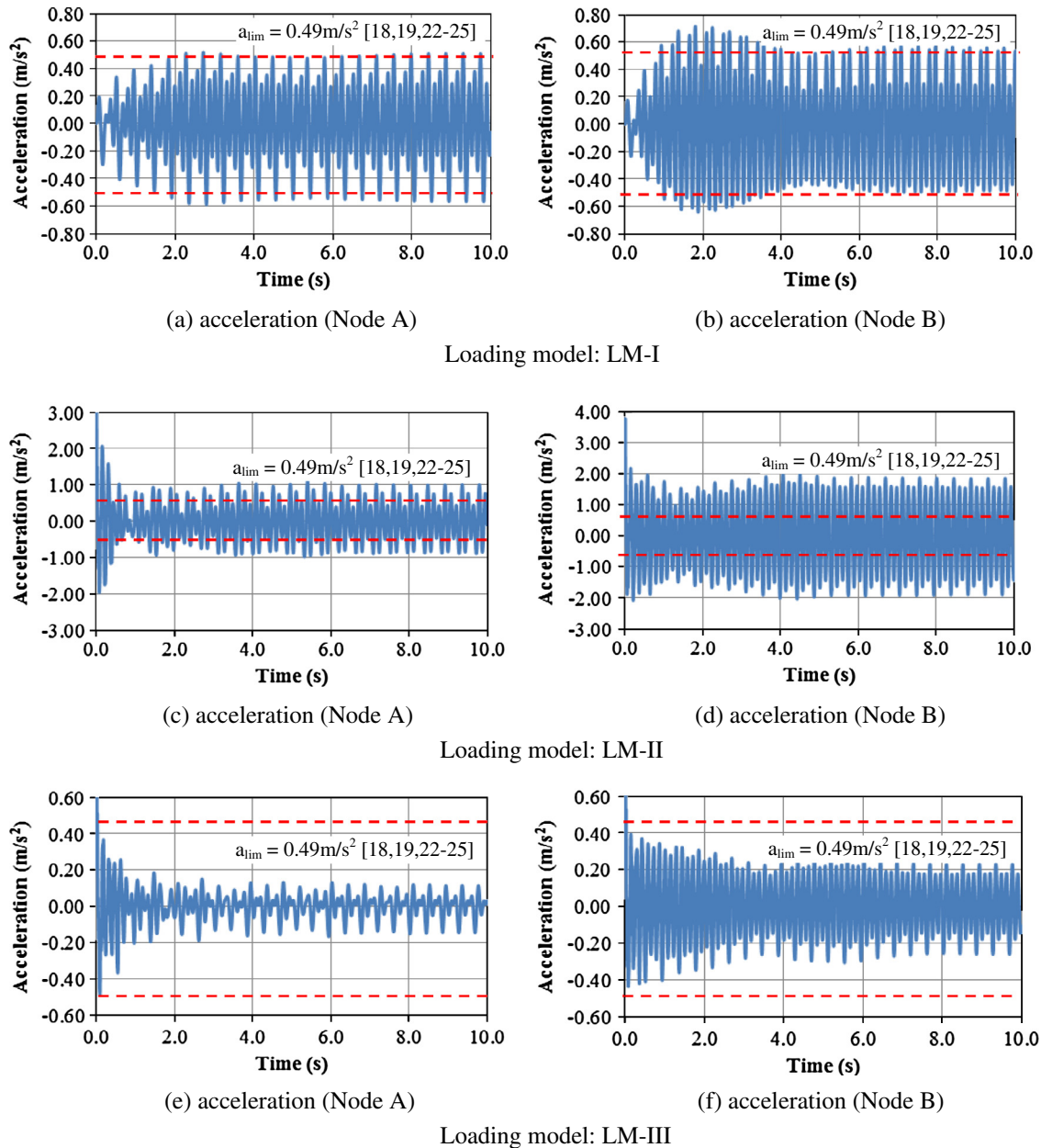
(a) acceleration (Node A)   (b) acceleration (Node B)

Loading model: LM-I

(c) acceleration (Node A)   (d) acceleration (Node B)

Loading model: LM-II

(e) acceleration (Node A)   (f) acceleration (Node B)

Loading model: LM-III

Fig. 13. Structural model displacements and accelerations. Steel–concrete: partial interaction. Beam-to-column connections: semi-rigid. Beam-to-beam connections: semi-rigid. Stud: 19 mm.

6. Assessment of the composite floor dynamic response

Firstly, the steel–concrete composite floor natural frequencies were determined with the aid of the numeric simulations and compared with frequency values obtained by AISC design recommendations [27]. The composite floor finite element fundamental frequency was equal to 6.06 Hz (f_{01} = 6.06 Hz: beam-to-column rigid/beam-to-beam flexible/total interaction) and the frequency value obtained by AISC recommendations [27] was equal to 6.17 Hz (f_{01} = 6.17 Hz). It is clear from the obtained results, that there is very good agreement between the finite element frequency values and the frequency values obtained by AISC [27]. It must be emphasised that the frequencies calculated by two different strategies correspond to the expected range for the investigated floor. Such fact validates the numeric model presented here, as well as the results and conclusions obtained throughout this investigation.

Considering the investigated composite floor natural frequencies, see Tables 2–5, a small difference between the numeric results

obtained with the use of total interaction or partial interaction (50%) can be observed. The largest difference between the natural frequencies was approximately equal to 5 to 7%, as presented in Tables 2–5 and Fig. 10. Fig. 11 presents the composite floor vibration modes when total and partial interaction situations were considered in the numerical analysis. It must be emphasised that the composite floor vibration modes did not present significant modifications when the connections' flexibility and steel–concrete interaction were changed and that the structural model presented vibration modes with a predominance of flexural effects, see Fig. 11.

The present study proceeded with the evaluation of the structural model performance in terms of human comfort and vibration serviceability limit states. The peak acceleration analysis was focused on aerobics and considered parameters carefully chosen to simulate this human rhythmic activity on the analysed floor (LM-I: T_c = 0.34 s, T_s = 0.10 s and K_p = 2.78). This way, Figs. 12 and 13 illustrate the dynamic response (accelerations) related to nodes

Table 6
Composite floor peak accelerations. Beam-to-column rigid connections. Investigated nodes: A to H (see Fig. 5).

LM	Studs	Beam-to-beam connections	Complete interaction a_p (m/s^2) Nodes				Partial interaction (50%) a_p (m/s^2) Nodes			
			A	B	C	D	A	B	C	D
I	19 mm	Rigid	0.23	0.12	0.12	0.23	0.30	0.25	0.25	0.30
		Semi-rigid	0.30	0.31	0.31	0.30	0.42	0.47	0.47	0.42
		Flexible	0.35	0.34	0.34	0.35	0.50	0.60	0.60	0.50
II	19 mm	Rigid	0.35	0.10	0.10	0.35	0.50	0.47	0.47	0.50
		Semi-rigid	0.40	0.46	0.46	0.40	0.79	0.97	0.97	0.79
		Flexible	0.60	0.57	0.57	0.60	1.32	1.35	1.35	1.32
III	19 mm	Rigid	0.10	0.10	0.10	0.10	0.16	0.10	0.10	0.16
		Semi-rigid	0.14	0.18	0.18	0.14	0.18	0.20	0.20	0.18
		Flexible	0.18	0.21	0.21	0.18	0.22	0.27	0.27	0.22
			E	F	G	H	E	F	G	H
I	19 mm	Rigid	0.02	0.06	0.06	0.02	0.20	0.04	0.04	0.20
		Semi-rigid	0.20	0.05	0.05	0.20	0.31	0.16	0.16	0.31
		Flexible	0.21	0.08	0.08	0.21	0.40	0.17	0.17	0.40
II	19 mm	Rigid	0.03	0.08	0.08	0.03	0.36	0.30	0.30	0.36
		Semi-rigid	0.34	0.12	0.12	0.34	0.54	0.39	0.39	0.54
		Flexible	0.37	0.13	0.13	0.37	0.80	0.70	0.70	0.80
III	19 mm	Rigid	0.08	0.04	0.04	0.08	0.09	0.05	0.05	0.09
		Semi-rigid	0.11	0.06	0.06	0.11	0.12	0.10	0.10	0.12
		Flexible	0.15	0.07	0.07	0.15	0.16	0.12	0.12	0.16

Limiting acceleration: a_{lim} = 0.49 m/s^2 (5%g – g: gravity) [18,19,22–25].

Table 7
Composite floor peak accelerations. Beam-to-column semi-rigid connections. Investigated nodes: A to H (see Fig. 5).

LM	Studs	Beam-to-beam connections	Complete interaction a_p (m/s^2) Nodes				Partial interaction (50%) a_p (m/s^2) Nodes			
			A	B	C	D	A	B	C	D
I	19 mm	Rigid	0.30	0.18	0.18	0.30	0.36	0.35	0.35	0.36
		Semi-rigid	0.41	0.40	0.40	0.41	0.52	0.51	0.51	0.52
		Flexible	0.54	0.50	0.50	0.54	0.58	0.65	0.65	0.58
II	19 mm	Rigid	0.60	0.40	0.40	0.71	0.71	0.59	0.59	0.71
		Semi-rigid	1.00	0.67	0.67	1.00	1.00	1.70	1.70	1.00
		Flexible	1.07	1.00	1.00	1.07	1.32	1.77	1.77	1.32
III	19 mm	Rigid	0.18	0.20	0.20	0.18	0.19	0.21	0.21	0.19
		Semi-rigid	0.20	0.22	0.22	0.20	0.19	0.24	0.24	0.19
		Flexible	0.20	0.27	0.27	0.20	0.27	0.30	0.30	0.27
			E	F	G	H	E	F	G	H
I	19 mm	Rigid	0.17	0.15	0.15	0.17	0.18	0.04	0.04	0.18
		Semi-rigid	0.30	0.04	0.04	0.30	0.30	0.27	0.27	0.30
		Flexible	0.30	0.05	0.05	0.30	0.32	0.28	0.28	0.32
II	19 mm	Rigid	0.33	0.25	0.25	0.33	0.50	0.30	0.30	0.50
		Semi-rigid	0.51	0.42	0.42	0.51	0.55	0.51	0.51	0.55
		Flexible	0.53	0.21	0.21	0.53	0.63	0.52	0.52	0.63
III	19 mm	Rigid	0.09	0.08	0.08	0.09	0.10	0.09	0.09	0.10
		Semi-rigid	0.10	0.10	0.10	0.10	0.12	0.11	0.11	0.12
		Flexible	0.20	0.12	0.12	0.20	0.16	0.14	0.14	0.16

Limiting acceleration: a_{lim} = 0.49 m/s^2 (5%g – g: gravity) [18,19,22–25].

A and B (see Fig. 5) when thirty-two people are practising aerobics on the composite floor. It is possible to verify that the dynamic actions resulting from aerobics generated peak accelerations higher than 5%g (a_{lim} = 0.49 m/s^2) [23,24,27–30], leading to a violation of the current human comfort criteria, as illustrated in Figs. 12 and 13.

When the LM-I (see Eq. (1)) was considered, the peak accelerations were equal to 0.60 m/s^2 (a_{max} = 0.60 m/s^2: beam-to-column connections rigid) and 0.65 m/s^2 (a_{max} = 0.65 m/s^2: beam-to-column connections semi-rigid), respectively, see Tables 6 and 7. This trend was confirmed in several other situations [1,6,16–22] in which the human comfort criterion was violated. On the other hand, these peak accelerations tend to drastically decrease when the floor dynamic response obtained on nodes E to H (Fig. 5) was compared to nodes A to D (Fig. 5). In this situation the human comfort criteria was not violated, see Tables 6 and 7.

The results also indicate that when the steel–concrete interaction degree (from total to partial) and the joint flexibility (rigid to flexible) decrease, the composite floor natural frequencies become smaller, see Tables 2–5, and the composite floor peak accelerations become larger, see Tables 6 and 7. This way, structural designers should be aware that the actual floor dynamic characteristics after construction can be very different from the designed one. This conclusion is important because the structure can become even more susceptible to excessive vibrations induced by human rhythmic activities.

It can be noted that the difference between the peak acceleration values is related to the nature of the loading models, see Tables 6 and 7. When the Loading Model I (LM-I) was considered in the analysis, the dynamic actions are not in phase on the composite floor, due to the fact that all variations which lead to the reduction of the dynamic action on the structure are embedded

in the coefficients K_p and CD. This way, the peak acceleration values are more realistic and in consonance with the design practice, see Tables 6 and 7.

On the other hand, the Loading Model II (LM-II) does not incorporate any variations which lead to the reduction of the dynamic loading on the floor (phase lags between the individuals and change of rhythm during the activity). In this situation the dynamic loads are in phase on the floor [27], and the peak acceleration values are overestimated and not realistic. However, the Loading Model III (LM-III) leads to very low peak accelerations, even considering a resonance situation. In this case the LM-III underestimates the effect of the human rhythmic dynamic loads. This fact is probably associated to the harmonic frequencies of the dynamic excitation and dynamic coefficients adopted in this model [30].

7. Conclusions

This paper presented the development of a design methodology centred on the finite element modelling of the dynamic behaviour of a typical steel–concrete composite floor of a commercial building subjected to human rhythmic activities (aerobics) aiming the evaluation and assessment of excessive vibrations and human comfort. The structural behaviour of the beam-to-column and beam-to-beam connections (rigid, semi-rigid and flexible joints) and also the stud connectors (from total to partial interaction cases) present in the investigated structural model were simulated in this analysis. The following conclusions can be drawn from the results presented in this study:

1. The influence of the connectors (Stud Bolts: 16 mm and 19 mm) on the values of the investigated steel–concrete composite floor's natural frequencies was very small when the steel–concrete interaction degree (from total to partial) was considered in the analysis. The largest difference was approximately equal to 5 to 7%.
2. When the steel–concrete interaction degree (from total to partial) and the connections flexibility (rigid to flexible) decrease, the composite floor natural frequencies become smaller. This fact is relevant because the system becomes more susceptible to excessive vibrations. Structural designers should be aware that the actual composite floor dynamic characteristics after construction can be very different from the designed one.
3. The composite floor vibration modes did not present significant modifications when the steel–concrete interaction and connections flexibility were changed. The investigated structure presented vibration modes with a predominance of flexural effects.
4. The peak acceleration values calculated based on the LM-I are more realistic and in consonance with the design practice. It must be emphasised that the load factors in the rhythmic crowd load model used in this loading model were determined based on a long series of experimental tests with individuals performing rhythmic and non-rhythmic activities and also probabilistic analyses.
5. The peak acceleration values obtained with the partial interaction degree (50%) between the steel and the concrete were always higher when compared with the model that considered total interaction (complete interaction). The maximum value found in this study was equal to 0.65 m/s^2 (a_p = 0.65 m/s^2 -> a_{lim} = 0.49 m/s^2: beam-to-column semi-rigid/beam-to-beam flexible/partial interaction).
6. The current investigation indicated that human rhythmic activities could induce the steel–concrete composite floors to reach unacceptable vibration levels and, in these situations, lead to a violation of the current human comfort criteria for these specific structures.

References

[1] Lopes EDC. Non-linear dynamical analysis of composite floors considering the effects of partial interaction and beam to column and beam to beam connections, PhD Thesis (In Portuguese). Civil Engineering Department. Pontifical Catholic University of Rio de Janeiro, PUC-Rio, Rio de Janeiro/RJ, Brazil. 2012.
[2] Labonnote N, Rønnquist A, Malo KA. Prediction of material damping in timber floors, and subsequent evaluation of structural damping. Mater Struct 2014. http://dx.doi.org/10.1617/s11527-014-0286-7. p 1–11.
[3] Setareh M. Evaluation and assessment of vibrations owing to human activity. In: Proceedings of the institution of civil engineers. vol. 165 (SB5). Structures and Buildings; 2012. p. 219–31.
[4] Setareh M. Vibration serviceability of a building floor structure. I: Dynamic testing and computer modelling. J Perform Constr Facil 2010;24:497–507. ASCE.
[5] Setareh M. Vibration serviceability of a building floor structure. II: Vibration, evaluation and assessment. J Perform Constr Facil 2010;24:508–18. ASCE.
[6] De Silva SS, Thambiratnam DP. Dynamic characteristics of steel-deck composite floors under human-induced loads. Comput Struct 2009;87: 1067–76.
[7] Smith AL, Hicks SJ, Devine PJ. Design of floors for vibrations: a new approach. SCI Publication. P354, Ascot, 2009.
[8] Saidi I, Haritos N, Gad EF, Wilson JL. Floor vibrations due to human excitation – damping perspective. In: Proceedings of the earthquake engineering in Australia. Canberra, Australia, CD-ROM; 2006. p. 1–8.
[9] Ebrahimpour A, Sack RL. A review of vibration serviceability criteria for floor structures. Comput Struct 2005;83(28–30):2488–94.
[10] Ellis BR, Littler JD. Response of cantilever grandstands to crowd loads. Part I: Serviceability evaluation. Struct Build 2004;157(SB4):235–41.
[11] Pavic A, Reynolds P, Waldron P, Bennett KJ. Critical review of guidelines for checking vibration serviceability of post-tensioned concrete floors. Cement Concr Compos 2001;23(1):21–31.
[12] Pavic A, Reynolds P. Experimental assessment of vibration serviceability of existing office floors under human-induced excitation. Exp Tech 1999;23(5):41–5.
[13] Dolan JD, Murray TM, Johnson JR, Runte D, Shue BC. Preventing annoying wood floor vibrations. J Struct Eng 1999;125(1):19–24.
[14] Smith I, Chui YH. Design of lightweight wooden floors to avoid human discomfort. Can J Civ Eng 1988;15(2):254–62.
[15] Tolaymat RA. A new approach to floor vibration analysis. Eng J AISC 1988;25(4):137–43.
[16] Gonçalves SG. Non-linear dynamic analysis of composite floors submitted to human rhythmic activities, MSc Dissertation (In Portuguese). Civil Engineering Post-graduate Programme, PGECIV. State University of Rio de Janeiro, UERJ, Rio de Janeiro/RJ, Brazil. 2011.
[17] Silva JGS da, Vellasco PCG da S, Andrade SAL de, Lima LRO de, Almeida RR de. Vibration analysis of long span joist floors when submitted to dynamic loads due to human activities. In: Proceedings of the 9th international conference on computational structures technology, CST 2008, Athens, Greece, CD-ROM; 2008. p. 1–11.
[18] Langer NA dos S, Silva JGS da, Vellasco PCG da S, Lima LRO de, Neves LF da C. Vibration analysis of composite floors induced by human rhythmic activities. In: Proceedings of the 12th international conference on civil, structural and environmental engineering computing, CC 2009, Funchal, Ilha da Madeira, Portugal, CD-ROM; 2009. p. 1–14.
[19] Lopes EDC, Silva JGS da, Andrade SAL de. Nonlinear dynamic analysis of steel-concrete composite floors submitted to human rhythmic dynamic actions. XXXV South American journeys of structural engineering, Rio de Janeiro/RJ, Brazil, CD-ROM; 2012. p. 1–13.
[20] Lopes EDC, Silva JGS da, Andrade SAL de. Vibration analysis of building composite floors submitted to human rhythmic activities. In: Nordic steel construction conference, NSCC 2012, Oslo, Norway, CD-ROM; 2012. p. 1–12.
[21] Loose JK. Dynamic analysis of composite floors (steel-concrete) submitted to human rhythmic activities. MSc Dissertation (In Portuguese). Civil engineering post-graduate programme. Federal University of Espirito Santo, UFES, Vitória/ES, Brazil. 2007.
[22] Mello AVA. Analysis of the effect of steel-concrete interaction on the dynamic response of composite floors, PhD Thesis (In Portuguese). Civil engineering department. Pontifical Catholic University of Rio de Janeiro, PUC-Rio, Rio de Janeiro/RJ, Brazil. 2009.
[23] Bachmann H, Ammann W. Vibrations in structures induced by man and machines, IABSE structural engineering document 3E, International Association for Bridges and Structural Engineering, ISBN 3-85748-052-X. 1987.
[24] Bachmann H, Ammann WJ, Deischl F, Eisenmann J, Floegl J, Hirsch GH, et al. Vibration problems in structures – practical guidelines", Basel (Switzerland): Institut für Baustatik und Konstruktion, Birkhäuser; 1995.

[25] Faisca RG. Characterization of dynamic loads due to human activities, PhD Thesis (In Portuguese), Civil Engineering Department, COPPE/UFRJ, Rio de Janeiro/RJ, Brazil. 2003.

[26] ANSYS Swanson Analysis Systems Inc. P.O. Box 65, Johnson Road, Houston, PA, 15342–0065. Release 11.0, SP1 UP20070830, ANSYS, Inc. is a UL registered ISO 9001:2000 Company. Products ANSYS Academic Research, Using FLEXlm v10.8.0.7 build 26147, Customer 00489194. 2007.

[27] Murray TM, Allen DE, Ungar EE. Floor vibrations due to human activity. Steel design guide series. American Institute of Steel Construction, AISC, Chicago, USA. 2003.

[28] International Standard Organization. Evaluation of human exposure to whole-body vibration, Part 2: human exposure to continuous and shock-induced vibrations in buildings (1–80 Hz), ISO 2631–2. 1989.

[29] International Organization for Standardzation. ISO 2631/1: evaluation of human exposure to whole-body vibration – Part 1: General requirements, Switzerland. 1985.

[30] Comité Euro-international du Béton. CEB-FIP: Bulletin d'information, N^0 209, England, London. 1993.

[31] Oliveira TJL. Steel to concrete composite floors with semi-rigid connections: non-linear static and dynamic, experimental and computational analysis, PhD Thesis (In Portuguese). COPPE/UFRJ, Federal University of Rio de Janeiro, Rio de Janeiro/RJ, Brazil. 2007.

[32] Carvalho LCV. Evaluation of semi-rigid bolted connections in steel structures. MSc Dissertation (In Portuguese). Civil engineering department. Pontifical Catholic University of Rio de Janeiro, PUC-Rio. Rio de Janeiro/RJ, Brazil. 1997.

[33] Ellobody E, Young B. Performance of shear connection in composite beans with profiled steel sheeting. J Constr Steel Res 2005;62:682–94.

[34] Tristão GA. Behaviour of shear connectors in composite steel-concrete beams with numerical analysis of the response, MSc Dissertation (In Portuguese). School of Engineering of Sao Carlos. University of São Paulo, São Carlos/SP, Brazil. 2002.

[35] David DL. Theoretical analysis and experimental shear connectors and composite beams consisting of profiles of cold-formed steel beams and slab precast. PhD Thesis, School of Engineering of São Carlos, University of São Paulo; 2007. p. 250.

[36] Varela WD, Battista RC. Control of vibrations induced by people walking on large span composite floor decks. Eng Struct 2011;33(9):2485–94.

[37] Clough RW, Penzien J. Dynamics of structures. McGraw-Hill; 1993. p. 634.